Assessment of the use of partitioning and interfacial tracers to determine the content and mass removal rates of nonaqueous phase liquids

Noordman, Wouter H.; Boer, Geert J. de; Wietzes, Pieter; Volkering, Frank; Janssen, Dick B.

Published in:
Environmental science & technology

DOI:
10.1021/es990098l

Environ. Sci. Technol. **2000**, *34,* 4301−4306

Assessment of the Use of Partitioning and Interfacial Tracers To Determine the Content and Mass Removal Rates of Nonaqueous Phase Liquids

WOUTER H. NOORDMAN,[†,‡] GEERT J. DE BOER,[†] PIETER WIETZES,[†] FRANK VOLKERING,[§,||] AND DICK B. JANSSEN*[,†]

Department of Biochemistry, Groningen Biomolecular Sciences and Biotechnology Institute, University of Groningen, Nijenborgh 4, 9747 AG Groningen, The Netherlands, and MTI Milieutechnologie, Nijmegen, The Netherlands

It was assessed whether partitioning and interfacial tracers can be used to determine the content and mass removal rate of nonaqueous phase liquid (NAPL) in porous media. Retardation factors for these tracers were determined for five different model matrices contaminated with hexadecane as NAPL. The retardation of the partitioning tracer 2,4-dimethyl-3-pentanol was correlated with the degree of NAPL saturation for four of the five matrices ($r^2 = 0.93$, $n = 8$). The observed retardation factors matched the retardation factors predicted with the independently determined hexadecane−water partitioning constant and the degree of NAPL saturation, indicating that this tracer may be used to estimate the degree of NAPL saturation of porous media. The mass removal rates of NAPL from columns packed with different matrices were determined by measuring the amount of hexadecane in the column effluent during elution with electrolyte solution. These removal rates differed over 3 orders of magnitude, dependent on the matrix used. The retardation of the interfacial tracer alkylbenzenesulfonate was higher for matrices with higher NAPL mass removal rates but was not correlated to the degree of NAPL saturation. This indicates that the retardation factors of alkylbenzenesulfonates in NAPL-contaminated media contain information related to the NAPL mass removal rates.

Introduction

The determination of the content and mass removal rates of nonaqueous phase liquids (NAPLs) in porous matrices is essential for soil remediation and risk assessment of sites contaminated with water-immiscible components. Recently, the use of partitioning and interfacial tracers for determination of the degree of NAPL saturation and the specific NAPL−water interfacial area has attracted attention (*1*−*4*). An advantage of the use of tracers over traditional methods is that it is noninvasive and yields an average value that refers to the entire flow field. In contrast, traditional ways of soil sampling require analysis of many samples to obtain a representative average value for a site because of site heterogeneity (*1*).

Compounds that have been used as partitioning tracers for the determination of the NAPL content or degree of NAPL saturation (S_n, L of NAPL/L of pore vol) of contaminated soil include alcohols (*1*, *3*, *5*, *6*), sulfur hexafluoride (*2*), fluorocarbon compounds (*7*, *8*), and the naturally occurring isotope ^{222}Rn (*9*). Partitioning tracers distribute between the NAPL and aqueous phases, causing retardation of these tracers relative to a conservative tracer. The tracers have been applied in both laboratory (*1*, *2*, *9*) and field situations (*5*, *6*, *9*) and have been used to determine levels of NAPL saturation S_n between 0.006 and 0.2. The level of NAPL saturation can be calculated from the retardation factor of a partitioning tracer by using eq 1 (*1*, *6*), provided that the retardation factor is determined solely by the degree of NAPL saturation and the NAPL−water partitioning constant, K_{nw} (g/L of NAPL phase)/(g/L of aqueous phase). Furthermore, the partitioning constant of the tracer must be independent of tracer concentration, and the mobile aqueous phase containing the tracers should contact all NAPL present:

$$R = 1 + K_{nw}\frac{S_n}{(1 - S_n)} \quad (1)$$

The K_{nw} values depend on the nature of the tracer and the NAPL. For alcohol tracers, K_{nw} increases with increasing tracer hydrophobicity and decreases with increasing NAPL hydrophobicity (*10*). The agreement that was generally observed between results obtained with tracer experiments and data from soil core sampling (*5*, *6*, *8*, *9*) suggests that the retardation of partitioning tracers indeed is determined by S_n and K_{nw}. However, a systematic study has not been conducted to determine whether this relation holds for NAPLs present in various porous matrices and at different surface area-to-volume ratios. Such a more rigorous demonstration would increase the reliability of this promising technique.

Surfactants such as linear alkylbenzenesulfonate (LAS, also known as sodium dodecyl benzenesulfonate, SDBS) tend to partition between the water−air or water−NAPL interface and bulk water and can thus be used as interfacial tracers (*3*, *4*, *11*, *12*). The retardation of these tracers gives information on the NAPL−water (or air−water) interfacial area. Interfacial tracers have also been applied in both laboratory (*4*, *11*, *12*) and field experiments (*3*). Verification of the relation between tracer retardation and interfacial area is complicated since the interfacial area is difficult to determine independently. The fact that interfacial areas calculated from tracer retardation factors corresponded to values that were calculated based on geometrical or thermodynamic considerations was used as a validation of the method (*4*, *13*). The NAPL−water interfacial area is believed to be important for many processes including NAPL dissolution (*14*), mass removal by transport (*3*, *4*), and biodegradation (*15*). Therefore, interfacial tracers may be useful for the characterization of NAPL-contaminated sites when their retardation factors would be correlated to processes, such as NAPL mass removal rates.

The goal of this work was to investigate how retardation of partitioning tracers is influenced by NAPL present in different porous media and to test the feasibility of interfacial tracers for determination of NAPL mass removal rates. The term mass removal rate is used in this paper to quantify the

* Corresponding author e-mail: D.B.Janssen@chem.rug.nl; telephone: +31-50 363 4209; fax: +31-50 363 4165.
† University of Groningen.
‡ Present address: NIZO Food Research, Ede, The Netherlands.
§ MTI Milieutechnologie.
|| Present address: TAUW Milieu, Deventer, The Netherlands.

10.1021/es990098l CCC: $19.00
Published on Web 09/13/2000

TABLE 1. Physical Properties of Matrices and Parameters Associated with Column Experiments

matrix	particle size (μm)	pore size (nm)	specific surface area (m^2/g)	specific surface area (cm^2/cm^3)[a]	bulk density (kg/L)	porosity (−)	size of 1 pore vol (mL)	interstitial velocity (m/d)
fine glass beads	40		7.3×10^{-2} [b]	2.9×10^{2}	1.3	0.40	10.6	2.8
coarse glass beads	1000		2.6×10^{-3} [b]	4.1×10^{1}	1.60	0.40	10.6	2.8
CPG-10-3000	60−125	300	7.8[c]	2.5×10^{4}	0.34	0.76	20.2	1.5
silica	40−63	6	4.9×10^{2} [c]	2.5×10^{6}	0.49	0.70	18.6	1.6
sea sand	100−300	ND	7.4×10^{-1} [d]	1.0×10^{4}	1.40	0.44	11.7	2.6

[a] a_{mw}, cm^2 of surface area/cm^3 of column vol, derived from specific surface area in m^2/g. [b] Value calculated by geometrical analysis from $4\pi r^2$ using 0.64 as the fraction of the total vol occupied by the spheres (random close packing). [c] As given by the manufacturer. [d] Determined by gas−physisorption using nitrogen.

elution of NAPL from columns packed with NAPL-contaminated matrices and includes all physical mass removal processes such as dissolution, detachment of NAPL microdroplets, or mobilization. Retardation factors for the tracers were determined with column studies in which both the degree of NAPL saturation and the NAPL mass removal rates varied independently. This was accomplished by using five model matrices with a large variation in particle size, pore size, and specific surface area. These matrices and the procedure for contaminating them with NAPLs were chosen in order to obtain homogeneously contaminated matrices with different specific NAPL−water interfacial areas and surface area-to-volume ratios. The retardation factors for the tracers were correlated with independently determined values for degrees of NAPL saturation and NAPL mass removal rates to evaluate the processes that determine tracer retardation.

Materials and Methods

Chemicals, Matrices, and Solutions. The tracer KBr was obtained from Merck (technical grade, Darmstadt, Germany). The tracers 4-methyl-2-pentanol (99% pure, MMP), 2,4-dimethyl-3-pentanol (99%, DMP), and sodium *n*-alkylbenzenesulfonate (technical grade, LAS) were obtained from Aldrich (Zwijndrecht, The Netherlands). Hexadecane (99%) was obtained from Acros (Geel, Belgium). Pure samples of 5-*n*-(*p*-sulfophenyl)undecane and 5-*n*-(*p*-sulfophenyl)dodecane were kindly provided by Dr. J. Tolls (*16*). Silica 60 (Merck), sea sand (Merck), controlled pore glass (CPG-10-3000, Electro Nucleonics Inc., Fairfield, NJ), fine glass beads (ABCR, Karlsruhe, Germany), and coarse glass beads (Fisher Scientific, Den Bosch, The Netherlands) were used as model matrices (Table 1). The buffered electrolyte solution contained 0.53 g/L $Na_2HPO_4 \cdot 12H_2O$, 0.14 g/L KH_2PO_4, 0.1 g/L $(NH_4)_2SO_4$, 0.02 g/L $MgSO_4 \cdot 7H_2O$, 390 μg/L $Ca(NO_3)_2$, 100 μg/L $FeSO_4 \cdot 7H_2O$, 5 μg/L $ZnSO_4 \cdot 7H_2O$, 5 μg/L HBO_3, 5 μg/L $CoCl_2 \cdot 6H_2O$, 5 μg/L $CuSO_4 \cdot 5H_2O$, 2 μg/L $MnSO_4 \cdot H_2O$, 2 μg/L $Na_2MoO_4 \cdot 2H_2O$, 1 μg/L $NiCl_2 \cdot 6H_2O$, 1 μg/L $Na_2WO_4 \cdot 2H_2O$, and 0.2 g/L NaN_3 to prevent biodegradation of the tracers and hexadecane. The pH was adjusted to 7.0. The tracer solution contained 10 mM KBr, 10 mM MMP, 10 mM DMP, and 500 mg/L LAS in electrolyte solution. The cmc of LAS is approximately 500 mg/L (*13*, *17*), implying that no micelles were present in the pulse-type column experiments.

Contamination of Matrices. Matrices were contaminated by the addition of 90−1200 μL of hexadecane to 50 g of matrix suspendend in 100 mL of pentane. After incubation for approximately 12 h, the pentane was gradually removed using a rotary evaporator. Since the volatility of pentane is high (boiling point under ambient pressure 35−36 °C) and reduced pressure was used, it can be assumed that pentane was completely removed. Columns packed with these materials had degrees of NAPL saturation (S_n) of 0.001−0.09 L of hexadecane/L of pore vol (Table 2). These degrees were relatively low as compared to those used by other investigators and were chosen to obtain hexadecane-contaminated matrices that resembled a residual NAPL. Since S_n could be determined accurately and reproducibly by GC after extraction of samples (100 mg) with isooctane, the method of contamination resulted in homogeneous NAPL distribution over the length of the columns.

TABLE 2. Degrees of NAPL Saturation (S_n), Mass Removal Rates of Hexadecane (v_n), and Retardation Factors for Tracers

matrix	S_n (L/L)	v_n (g/pore vol)	retardation factors DMP	LASa	LASb
fine glass beads	0		1.01	1.44	2.43
	2.2×10^{-2}	2.2×10^{-8}	1.10	a	a
coarse glass beads	0		0.97	1.06	1.19
	2.3×10^{-2}	1.1×10^{-8}	1.22	1.19	1.55
CPG-10-3000	0		0.99	1.04	1.11
	3.8×10^{-3}	1.6×10^{-7}	1.09	1.14	1.47
	1.7×10^{-2}	1.0×10^{-6}	1.20	1.06	1.34
	2.3×10^{-2} [b]			1.03	1.24
silica	0		2.96	1.26	1.74
	9.8×10^{-4}	5.9×10^{-7}	2.60		
	4.0×10^{-3}	2.7×10^{-6}	5.37	>20[c]	>20[c]
	1.2×10^{-2}	8.1×10^{-6}	9.60	>20[c]	>20[c]
sea sand	0		1.02	1.23	1.61
	2.1×10^{-2}	1.7×10^{-6}	1.27		
	2.7×10^{-2}	3.6×10^{-6}	1.28	5	6
	5.9×10^{-2}	1.9×10^{-6}	1.57	5	6
	8.5×10^{-2} [b]		1.75		

[a] Not measurable since LAS caused clogging of a column packed with contaminated fine glass beads. The tracer was omitted in this experiment. [b] Experiment with a sampling frequency of >16 data points per pore vol. [c] No breakthrough within 20 pore vol.

NAPL−Water Partitioning Constants. The NAPL−water partitioning constants (K_{nw}) of MMP and DMP were determined by extraction of 100 mL of aqueous solutions containing 1 mM MMP and 1 mM DMP or 10 mM MMP and 10 mM DMP with either 1 or 10 mL of hexadecane. After equilibration and centrifugation (3000 rpm, 15 min), the aqueous concentrations of MMP and DMP were determined in triplicate. The partitioning constants for MMP and DMP were 1.4 ± 0.2 and 11 ± 2, respectively. These values are in accordance with literature data (*3*, *6*, *10*). The aqueous phase and organic phase concentrations were linearly related in the tested range between 0.5 and 9 mM ($r^2 = 0.98$, $n = 4$).

Column Studies. Stainless steel columns (7.0 cm in length, 2.2 cm i.d., Alltech) were dry packed in incremental steps, either with hexadecane-contaminated material or with uncontaminated material. The NAPL distribution and degree of NAPL saturation did not change during packing, since S_n was low and hexadecane was tightly attached to the matrices. Electrolyte solution was delivered to the column in upward flow using an HPLC single piston pump. Stainless steel tubing (0.8 mm i.d.) was used for all connections. After saturating the columns by flushing with 100 mL of electrolyte solution at a flow rate of 0.1 mL/min, the amount of hexadecane in

the effluent was determined in three 7-mL effluent fractions. The bulk density (ρ, kg/L) and the porosity (θ, −) were determined gravimetrically. The flow rate during subsequent tracer experiments was 0.3 mL/min. The resulting interstitial velocities are listed in Table 1. An injection loop was used to inject 2.73 mL of tracer solution into the column. The column effluent was directed to a fraction collector and analyzed for bromide, MMP, DMP, and LAS for up to 25 pore vol. Immediately afterward the flow was decreased to 0.1 mL/min, and the amount of hexadecane was determined in one 7-mL effluent fraction. In one independent experiment with hexadecane-contaminated silica (S_n = 0.007), the amount of hexadecane in the effluent was determined for 26 pore vol with a 6-h interruption of the flow after 21 pore vol of elution.

Analytical Procedures. The specific surface area of sea sand was determined by gas-physisorption using nitrogen. The amounts of hexadecane in effluent samples and in the matrices were determined by GC-FID after extraction with isooctane. The aqueous bromide concentrations were determined using a colorimetric assay (*18*). Aqueous MMP and DMP concentrations were analyzed by GC-FID after extraction with pentane. LAS was analyzed using reversed-phase HPLC. Since LAS consists of multiple components that differ in hydrophobicity and interfacial properties, the two major peaks in the chromatogram were integrated. Each peak corresponded to components of uniform hydrophobicity. These components, referred to as LASa and LASb, coeluted with the pure LAS components 5-*n*-(*p*-sulfophenyl)undecane and 5-*n*-(*p*-sulfophenyl)dodecane, respectively. This observation together with the comparison of our chromatogram with the chromatogram reported by Nakae et al. (*19*) suggests that LASa and LASb contain 4-, 5-, and 6-*n*-(*p*-sulfophenyl)-undecane and 4-, 5-, and 6-*n*-(*p*-sulfophenyl)dodecane, respectively. The HPLC setup consisted of a Spark Basic Marathon autosampler (Spark Holland BV, Emmen, The Netherlands) with an injection volume of 40 μL, a Merck L-6200 pump (Hitachi, Ltd., Tokyo, Japan), a Chromsphere PAH 100 mm column (Chrompack, Bergen op Zoom, The Netherlands), and a Merck L-4200 UV−Vis detector (228 nm, Hitachi). Mobile phase A was a 10 mM aqueous sodium acetate buffer at pH 4.1, and mobile phase B was methanol. Gradient elution was performed by linearly changing the composition of the mobile phase from 66% phase B to 80% phase B in 8 min, followed by 8 min at 80% phase B, using a flow rate of 0.5 mL/min.

Quantitative Analysis. Retardation factors were calculated from the first central moment corrected for a finite pulse (*20*). In all experiments, except for those with silica, the retardation factor for bromide was used to calculate the pore volume. For columns packed with silica, the retardation factor for bromide was less than 1 due to ion exclusion. Therefore, the elution times for the tracers for these columns were converted to pore volume using the porosity. The NAPL mass removal rates v_n (g of hexadecane/pore vol) were determined as the product of the amount of hexadecane in the column effluent (C, g of hexadecane/L) and the water content of the column (L/pore vol, Table 1). NAPL−water interfacial areas were calculated from retardation factors for the interfacial tracer LASb by using the relation $a_{nw} = (R - R_0)\theta/K_i$ (*3*, *12*). The interfacial adsorption coefficients K_i were obtained as described by Saripalli et al. from the interfacial adsorption isotherm of LAS with decane using the estimated maximal effluent concentration for LAS (*12*) and were found to be approximately 8×10^{-4} cm.

Results and Discussion

NAPL Mass Removal Rates. To allow correlation of interfacial tracer retardation with NAPL mass removal rates, the rate of NAPL removal from contaminated matrices was determined. This was accomplished by measuring the amount of hexadecane in column effluents (g/L) during continuous flow operation of columns immediately before and after the tracer experiments for all matrices. These hexadecane levels exceed the aqueous solubility of 3.6×10^{-6} g/L (*21*) for columns packed with contaminated CPG-10-3000, sea sand, and silica by a factor 2−15, 42−87, and 9−120, respectively, and were slightly lower than the solubility for the fine and coarse glass beads. For one column packed with contaminated silica (S_n = 0.007), the amount of hexadecane in the column effluent was determined during continuous elution with electrolyte solution for 21 pore vol. This amount remained constant at $(3.9 \pm 0.9) \times 10^{-4}$ g/L. After a subsequent interruption of the flow for 6 h, the amount temporary increased to 4×10^{-3} g/L. This temporary increase indicates that the rate of mass transfer of hexadecane from the immobile to the mobile phase limits mass removal from the column (*22*). The results show that mass transfer of hexadecane from the immobile to the aqueous phase was not limited by its solubility. However, the removed amounts of hexadecane were low since a separate nonaqueous phase was not visible in the effluent and since the percentage that was removed from the columns was smaller than 0.2% of the amount initially present. This implies that the NAPL was not completely mobile but that individual microdroplets were occasionally detached from the immobile NAPL, which also may explain the observed rate-limited mass removal. The rate of detachment is likely to depend on the NAPL−water interfacial area a_{nw} (cm^2 of interface × cm^{-3} of unit column vol), which was previously observed for the solubilization of residual NAPLs present in water-wet media (*14*).

NAPL removal rates (v_n, g of hexadecane eluted/eluted pore vol) were calculated from the amount of hexadecane in the effluent (Table 2). This removal rate is directly proportional to the mass transfer rate of hexadecane from the immobile to the mobile phase under the specified conditions for two reasons. First, the flow interruption experiment showed that mass removal from the columns was limited by the rate of mass transfer from the immobile to the mobile phase. Second, the residual amounts of hexadecane in the matrix samples taken after the experiment from the top and bottom of the columns were not significantly different from the residual amount in samples of the mixed column content. The NAPL mass removal rates differed by 3 orders of magnitude, dependent on the matrix used (Table 2). No correlation existed between v_n and S_n (Figure 1A) or between v_n and the particle size for the whole data set. However, v_n increased with increasing specific surface area of the matrices a_{mw}/θ (cm^2 of surface × cm^{-3} of pore vol, Figure 1B). High a_{mw} values were observed for matrices with high porosities or small pore sizes, i.e., for matrices with high internal surface areas.

The dependency of the mass removal rate v_n on the specific surface area a_{mw} of the matrix can be understood by realizing that the procedure used to contaminate the matrices yields NAPL-wetted matrices. When the NAPL does not coat the entire surface area of the matrix, such as in the experiments with silica where the amount of NAPL present was smaller than the amount required to create monolayer coverage, a higher initial S_n value results in a higher NAPL−water interfacial area and a higher mass removal rate (Figure 1A). When the NAPL coats the entire matrix, a higher initial S_n value only results in an increased film thickness, which does not affect the mass removal rate. This was observed for sea sand (Figure 1A). Therefore, provided that no mobilization occurs, the value for the mass removal rate v_n is expected to increase with increasing S_n until the NAPL coats the entire matrix. The maximal value for v_n should then be determined by the surface area of the matrix a_{mw}/θ. This was indeed observed (Figure 1B).

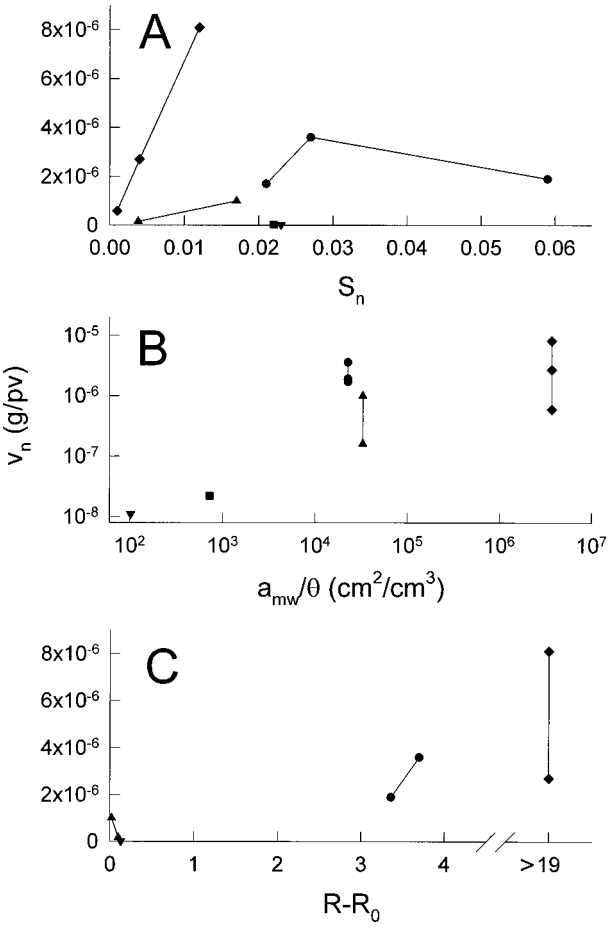

FIGURE 1. Rates of NAPL mass removal from the columns packed with fine glass beads (■), coarse glass beads (▼), CPG-10-3000 (▲), sea sand (●), and silica (◆). The NAPL mass removal rates v_n are shown as a function of NAPL saturation (A), specific matrix−water surface area (B), and retardation of the interfacial tracer LASa (C). The quantity a_{mw}/θ in panel B denotes the specific matrix−water surface area expressed as matrix−water surface area per pore vol (cm^2 cm^{-3}). The value of $R - R_0$ in panel C quantifies the part of the retardation of the interfacial tracer that was caused by the presence of the NAPL. Lines connect the data for each type of matrix.

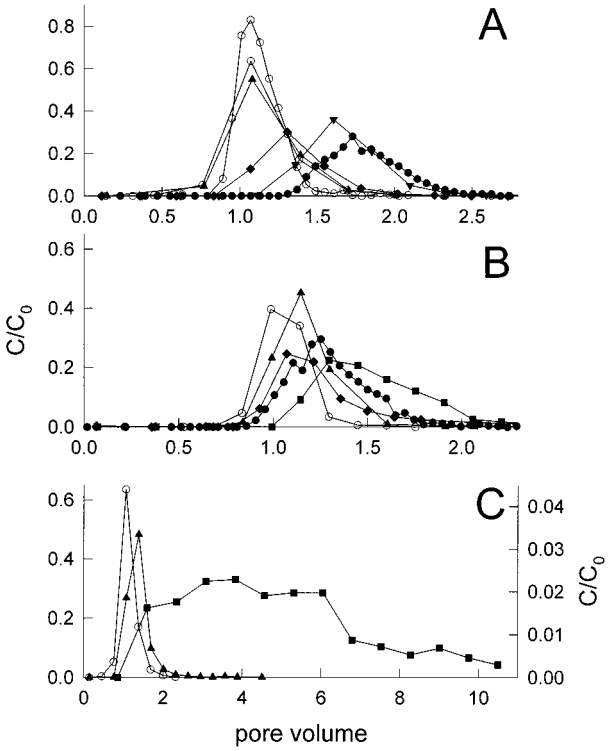

FIGURE 2. Selected breakthrough curves for tracers. (A) Breakthrough curves for bromide (○, two experiments) and DMP (▲, $S_n = 0$; ◆, $S_n = 0.027$; ▽, $S_n = 0.059$; ●, $S_n = 0.085$) through hexadecane-contaminated sea sand. (B) Breakthrough curves for bromide (○) and LASa (▲, $S_n = 0$; ■, $S_n = 0.0038$; ◆, $S_n = 0.017$; ●, $S_n = 0.023$) through hexadecane-contaminated CPG-10-3000. (C) Breakthrough curves for bromide (○, left *Y*-axis) and LASa (▲, $S_n = 0$, left *Y*-axis; ■, $S_n = 0.059$, right *Y*-axis) through hexadecane-contaminated sea sand.

Taken together, it can be concluded that the mass removal of hexadecane was rate-limited and strongly matrix-dependent. Higher mass removal rates were observed for matrices with high a_{mw}, i.e., matrices with high porosities and small pore sizes. Both the degree of NAPL saturation and mass removal rate remained constant during the tracer experiments. Therefore, this experimental setup was suitable to determine the dependency of tracer retardation on the degree of NAPL saturation and mass removal rate.

Tracer Studies. The shapes of breakthrough curves for the conservative tracer potassium bromide were sigmoidal and did not show tailing (Figure 2), indicating that the columns were packed homogeneously and that physical nonequilibrium effects were absent. Preliminary experiments using columns packed with contaminated sea sand showed that transport of the partitioning tracers was independent of the presence of other tracers. Subsequent tracer experiments were performed with a mixture of tracers. Total recovery of the tracers typically was between 80 and 110%, except for experiments with contaminated silica, where LAS did not break through during the experiment, and with contaminated sea sand, where due to tailing only 40% of the LAS tracer was recovered within 12 pore vol after the tracer pulse. Since effluent fractions were generally analyzed until the concentration of tracers was below $C/C_0 < 0.001$, the presence of tailing would always have been noticed. Therefore, the deviations of the mass balances from 100% was not caused by missing the lower concentrations in the distal portions of the BTC, which would also have led to an underestimation of the retardation factors. Deviations of the mass balances from 100% also did not result from the relatively low sampling frequency in some breakthrough curves, since all fractions containing significant amounts of tracers were analyzed. Most experiments were performed with a sampling frequency of approximately 3−5 data points per pore volume. Experiments with sampling frequency of more than 16 data points per pore volume were performed for bromide and DMP with contaminated sea sand (Figure 2A, Table 2) and for bromide and LAS with contaminated CPG-10-3000 (Figure 2B, Table 2). The shape of the breakthrough curves, the mass balances, and the retardation factors from these experiments agreed with data from experiments with a lower sampling frequency at a similar S_n (Figure 2, Table 2), indicating that the sampling frequencies used in this study were sufficient to allow estimation of the retardation factors.

Partitioning Tracers. To determine whether the retardation of the partitioning tracer was determined solely by the degree of NAPL saturation of a column, breakthrough curves of the tracers were measured with five matrices contaminated to different degrees of hexadecane saturation S_n (e.g., Figure 2A). At low S_n, as in the experiments described here, eq 1 reduces to $R = 1 + K_{nw}S_n$ and thus predicts a linear relation between R and S_n. The shapes of the breakthrough curves for the partitioning tracers through the uncontaminated and contaminated columns did not show tailing, indicating that nonequilibrium effects were absent under the conditions

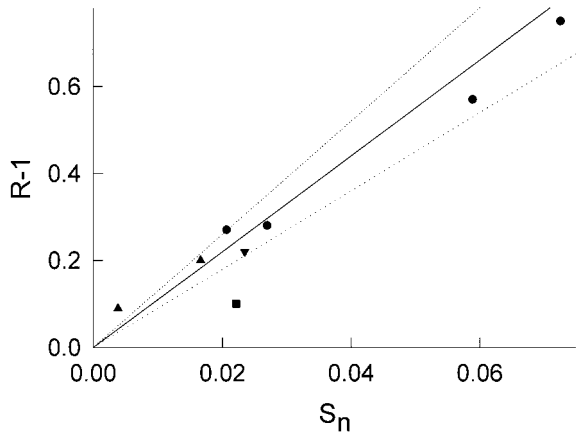

FIGURE 3. Dependence of retardation factors for the partitioning tracers on the degree of NAPL saturation of the matrix. Fine glass beads (■), coarse glass beads (▼), CPG-10-3000 (▲), and sea sand (●) were used as matrices. The solid line gives predicted retardation factors for DMP using the experimentally determined K_{nw} and S_n; the dotted lines give ±1 SD.

used. This also implies that K_{nw} was independent of tracer concentration, as was also determined with the batch partitioning studies. Nonlinear sorption or partitioning would have produced skewed breakthrough curves (*23*). The retardation factors R_0 for the partitioning tracers with the uncontaminated matrices, except with silica, were close to unity (Table 2), indicating that sorption of these tracers to the matrix was negligible. The retardation factors for MMP with the contaminated matrices were close to unity due to the low K_{nw} and S_n. Therefore, this tracer was not useful to determine degree of NAPL saturation in these matrices and was omitted from further analysis.

The experimentally determined retardation factors for the partitioning tracer DMP were indeed linearly correlated with S_n ($r^2 = 0.93$, $n = 8$, silica data omitted). Additionally, the retardation factors corresponded well to the retardation factors as calculated from the independently determined K_{nw} and S_n (Figure 3). This provides convincing evidence that the retardation of DMP is determined by NAPL−water partitioning and implies that levels of NAPL saturation can be determined from retardation factors for this tracer without the need to account for the porosity of the soil or the presence of micropores.

Interfacial Tracers. The shapes of the breakthrough curves for the interfacial tracers through the uncontaminated matrices did not show tailing, indicating that transport was not influenced by nonlinear sorption. The breakthrough curves for LAS through most of the contaminated matrices also did not show tailing (Figure 2B). However, significant tailing was observed for experiments using contaminated sea sand, reflecting the nonlinear nature of the interfacial NAPL−water adsorption isotherm (Figure 2C). It was surprising that tailing was observed with sea sand and not with CPG-10-3000, given the similar a_{mw}/θ values for these matrices. Not only was more tailing observed with sea sand than with CPG-10-3000, also a higher v_n and higher retardation factors for the interfacial tracers were observed with this matrix (Table 2). Presumably, the a_{nw}/θ with sea sand was higher than with CPG-10-3000, despite the similarity in a_{mw}/θ.

Retardation factors for the more hydrophobic LASb were higher than for LASa, indicating that NAPL−water interfacial adsorption increased with increasing tracer hydrophobicity. This also shows that it is appropriate to determine breakthrough of LAS components instead of LAS as total surfactant (*24*). The retardation factor for the LAS tracers varied from 1.06 to >20 for the four model matrices at a similar degree of NAPL saturation S_n of approximately 2×10^{-2} (Table 2), indicating that retardation of these tracers was not determined by NAPL−water partitioning. Instead, a positive correlation was observed between retardation of the interfacial tracers and the independently determined NAPL mass removal rate v_n (Table 2, Figure 1C). For instance, the retardation factors for LASa and LASb were low for the experiments with the matrices with low v_n (coarse glass beads and CPG-10-3000) and high for the matrices with high v_n (sea sand and silica).

A correlation between retardation of LAS and NAPL mass removal rate was expected since both the retardation of LAS (*4*) and the NAPL dissolution rate (*3*, *14*, *25*) depend on the specific NAPL−water interfacial area a_{nw}. However, several factors may disturb the correlation between v_n and R. For instance, the nonlinearity of the NAPL−water interfacial isotherm may cause LAS retardation to be nonproportional to a_{nw} (*3*). Also, the viscosity, buoyancy, and capillary forces that determine whether mass removal of NAPL occurs by mobilization (*26*) are not strictly related to a_{nw}. The observed correlation of the retardation factors for the interfacial tracers with v_n also explains the increase in v_n with increase in a_{mw}/θ (Figure 1B) given the proposed dependence of a_{nw} on a_{mw} for the types of contaminated matrices used in this study.

Estimates for the specific NAPL−water interfacial areas a_{nw} were determined from retardation factors for the interfacial tracer LASb. The estimated NAPL−water interfacial areas a_{nw} for the experiments with contaminated coarse glass beads and CPG-10-3000 were 1×10^2 and $2-3 \times 10^2$ cm^2 cm^{-3}, respectively. No reliable value could be derived for the experiments with contaminated sea sand, since the maximal effluent concentrations of the interfacial tracers in these experiments were much smaller that the range in which the relation between K_i and surfactant concentration was established (*12*). A comparison of the estimated values for a_{nw} with a_{mw} values (Table 1) indicates that CPG-10-3000 was not fully coated with hexadecane since the a_{nw} values were 2 orders of magnitude lower than the specific surface area a_{mw}. The coarse glass beads could have been completely covered. The estimated value for a_{nw} for coarse glass beads even was somewhat higher than the value for a_{mw} estimated from geometrical analysis (Table 1), which was also observed by Kim et al. (*13*) and was attributed to particle size heterogeneity and surface roughness that lead to an underestimation of a_{mw}. The estimated a_{nw} values were similar to a_{nw} values found for NAPLs in practical situations (*3*) and are in agreement with data for NAPL-wetted media (*12*), albeit our values were obtained at lower levels of NAPL saturation S_n. The ratio of interfacial area to volumetric NAPL content, calculated as $a_{nw}/S_n\theta$ (*3*), ranged from 1×10^4 cm^{-1} (sea sand) to 1×10^5 cm^{-1} (CPG-10-3000). These ratios were similar to those determined using these tracers in a field experiment (*3*). This analysis indicates that the type of NAPL contamination present in sea sand and CPG-10-3000 can also be encountered in field-contaminated soil, especially in smear zones (*3*).

The results show that retardation factors for LAS can provide qualitative information about NAPL mass removal rates since strong retardation of these interfacial tracers was correlated with high NAPL mass removal rates under the conditions employed in this work. Further work is needed to establish whether this correlation is also observed in situations where the NAPL contamination is present in water-wetted matrices, in situations where the NAPL is a multicomponent mixture, and under conditions where the NAPL is mobile. Saripalli et al. have shown that LAS retardation increases following NAPL mobilization (*4*), probably as a result of the increase in a_{nw} that accompanied the formation of emulsions during NAPL mobilization.

Silica. With contaminated silica, the retardation factors for both the partitioning tracer and the interfacial tracers were considerably larger than with all other matrices at similar S_n (Table 2). This strong retardation likely was caused by the surface area to volume ratio of the NAPL film that was expected to be exceptionally large due to the large specific surface area of silica (Table 1). The strong retardation of DMP suggests that this tracer behaved to some extent as an interfacial tracer. This is very well possible since amphiphilic alcohols are frequently used as cosurfactants and air−water interfacial adsorption of alcohols (*n*-hexanol to *n*-nonanol) caused significant retardation in unsaturated porous media (*27*). Since the specific surface area of silica is much larger than the surface areas of soil or aquifer material, interfacial adsorption of DMP is not expected to influence its retardation in soil contaminated with NAPL.

Implications for Field Application. The NAPLs employed in this study gave insight into the physical processes that determine tracer retardation. Although the NAPLs employed in this study may not always be representative of NAPLs present in practical situations, the results corroborate the possibility to use partitioning tracers to determine the degree of NAPL saturation by showing that retardation factors depend on K_{nw} and S_n and are independent of matrix properties such as pore size and porosity and of the surface area to volume ratios of the NAPL. The experimental data suggest that interfacial tracers may be used not only to determine a_{nw} values but also to characterize NAPL mass removal rates, at least for NAPLs that wet matrices.

Acknowledgments

This project was financed by the Dutch Research Program for In Situ Remediation (NOBIS) under Contract 95-1-09b. P. Peeters (van der Sluijs Tankopslag B.V.), H. A. G. M. Menning (Haskoning B.V.), A. Schaminee, and J. Tolls (RITOX,University of Utrecht) are acknowledged for their contributions.

Notation

a_{nw}	specific NAPL−water interfacial area, cm^2 of interface/cm^3 of unit column vol
a_{mw}	specific surface area for a matrix, cm^2 of interface/cm^3 of unit column vol
C	concentration of tracers or hexadecane in the effluent, g/L aqueous phase
C_0	concentration of tracer in the influent, g/L aqueous phase
K_{nw}	NAPL−water partitioning constant, (g/L NAPL phase)/(g/L aqueous phase)
R	retardation factor for a tracer with the contaminated matrix
R_0	retardation factor for a tracer with the uncontaminated matrix
S_n	degree of NAPL saturation, L of NAPL/L of pore vol
v_n	mass removal rate, g of hexadecane removed/pore vol
ρ	bulk density, kg of matrix/L of column vol
θ	porosity, L of pore vol/L of column vol

Literature Cited

(1) Jin, M.; Delshad, M.; Dwarakanath, V.; McKinney, D. C.; Pope, G. A.; Sepehrnoori, K.; Tilburg, C. E.; Jackson, R. E. *Water Resour. Res.* **1995**, *31*, 1201−1211.

(2) Wilson, R. D.; Mackay, D. M. *Environ. Sci. Technol.* **1995**, *29*, 1255−1258.

(3) Annable, M. D.; Jawitz, J. W.; Rao, P. S. C.; Dai, D. P.; Kim, H.; Wood, A. L. *Ground Water* **1998**, *36*, 495−502.

(4) Saripalli, K. P.; Kim, H.; Rao, P. S. C.; Anable, M. D. *Environ. Sci. Technol.* **1997**, *31*, 932−936.

(5) Jawitz, J. W.; Annable, M. D.; Rao, P. S. C.; Rhue, R. D. *Environ. Sci. Technol.* **1998**, *32*, 523−530.

(6) Annable, M. D.; Rao, P. S. C.; Hatfield, K.; Graham, W. D.; Wood, A. L.; Enfield, C. G. *J. Environ. Eng.* **1998**, *124*, 498−503.

(7) Studer, J. E. In *In Situ and On Site Bioremediation*; Alleman, B. C., Leeson, A., Eds.; Battelle Press: Columbus, OH, 1997; Vol. 4 (2), pp 345−351.

(8) Deeds, N. E.; Pope, G. A.; McKinney, D. C. *Environ. Sci. Technol.* **1999**, *13*, 2745−2751.

(9) Hunkeler, D.; Hoehn, E.; Höhener, P., Zeyer, J. *Environ. Sci. Technol.* **1997**, *31*, 3180−3187.

(10) Dwarakanath, V.; Pope, G. A. *Environ Sci. Technol.* **1988**, *32*, 1662−1666.

(11) Kim, H.; Rao, P. S. C.; Annable, M. D. *Water Resour. Res.* **1997**, *33*, 2705−2711.

(12) Saripalli, K. P.; Rao, P. S. C.; Annable, M. D. *J. Contam. Hydrol.* **1998**, *30*, 375−391.

(13) Kim, H.; Rao, P. S. C.; Annable, M. D. *J. Contam. Hydrol.* **1999**, *40*, 79−94.

(14) Powers, S. E.; Abriola, L. M.; Weber, W. J., Jr. *Water Resour. Res.* **1994**, *30*, 321−332.

(15) Ortega-Calvo, J.-J.; Alexander, M. *Appl. Environ. Microbiol.* **1994**, *60*, 2643−2646.

(16) Tolls, J.; Haller, M.; De Graaf, I.; Thijssen, M. A. T. C.; Sijm, D. T. H. M. *Environ. Sci. Technol.* **1997**, *31*, 3426−3431.

(17) Van Os, N. M., Haak, J. R., Rupert, L. A. M., Eds. *Physicochemical properties of selected anionic, cationic, and nonionic surfactants*; Elsevier: Amsterdam, 1993.

(18) Bergmann, J. G.; Sanik, J. *Anal. Chem.* **1957**, *29*, 241−243.

(19) Nakae, A.; Tsuji, K.; Yamanaka, M. *Anal. Chem.* **1981**, *53*, 1818−1821.

(20) Das, B. S.; Kluitenberg, G. J. *Soil Sci. Soc. Am. J.* **1996**, *60*, 1724−1731.

(21) Schwarzenbach, R. P.; Gschwend, P. M.; Imboden, D. M. *Environmental Organic Chemistry*, 1st ed.; John Willey & Sons: New York, 1993.

(22) Pennell, K. D.; Abriola, L. M.; Weber, W. J. *Environ. Sci. Technol.* **1993**, *27*, 2332−2340.

(23) Berglund, S. *J. Contam. Hydrol.* **1995**, *18*, 199−220.

(24) Field, J. A.; Istok, J. D. *Environ. Sci. Technol.* **1998**, *32*, 3836−3837.

(25) Abriola, L. M.; Dekker, T. J.; Pennell, K. D. *Environ. Sci. Technol.* **1993**, *27*, 2341−2351.

(26) Pennell, K. D.; Pope, G. A.; Abriola, L. M. *Environ. Sci. Technol.* **1996**, *30*, 1328−1335.

(27) Kim, H.; Annable, M. D.; Rao, P. S. C. *Environ. Sci. Technol.* **1998**, *32*, 1253−1259.

Received for review January 27, 1999. Revised manuscript received July 19, 2000. Accepted July 24, 2000.

ES990098L